PHYSICAL REVIEW A **93**, 021401(R) (2016)

Two-to-one Auger decay of a double L vacancy in argon

M. Žitnik,[1,2] R. Püttner,[3] G. Goldsztejn,[4,5] K. Bučar,[1] M. Kavčič,[1] A. Mihelič,[1] T. Marchenko,[4,5] R. Guillemin,[4,5] L. Journel,[4,5] O. Travnikova,[4,5] D. Céolin,[6] M. N. Piancastelli,[4,5,7] and M. Simon[4,5,6]

[1]*J. Stefan Institute, Jamova 39, SI-1000 Ljubljana, Slovenia*

[2]*Faculty of Mathematics and Physics, University of Ljubljana, Jadranska 19, SI-1000 Ljubljana, Slovenia*

[3]*Institut für Experimentalphysik, Freie Universitat Berlin, Arnimallee 14, D-14195 Berlin-Dahlem, Germany*

[4]*Sorbonne Université, UPMC Université Paris 06, UMR No. 7614, LCPMR, 75005 Paris, France*

[5]*CNRS, UMR No. 7614, LCPMR, 75005 Paris, France*

[6]*Synchrotron SOLEIL, L'Orme des Merisiers, Saint Aubin, BP 48, F-91192 Gif-sur-Yvette Cedex, France*

[7]*Department of Physics and Astronomy, Uppsala University, PO Box 516, 75120 Uppsala, Sweden*

(Received 14 November 2015; published 1 February 2016)

We have observed L_{23}^2-M^3 Auger decay in argon where a double vacancy is filled by two valence electrons and a single electron is ejected from the atom. A well-resolved spectrum of these two-to-one electron transitions is compared to the result of the second-order perturbation theory and its decay branching ratio is determined.

DOI: 10.1103/PhysRevA.93.021401

Even in atomic systems, photoexcitation and decay dynamics can be complex, calling for the solution of a many-body problem. A well-known type is multielectron excitation-ionization processes triggered by charged-particle collisions, e.g., quadruelectronic recombination where three bound electrons are excited upon capture of an incident electron [1], or single-photon absorption resulting, for example, in triple ionization of the Li atom [2] or simultaneous creation of vacancies at two different atoms in the molecule [3]. The core-hole lifetime (on the order of femtoseconds) is often much longer than the escape time of electrons (on the order of attoseconds) and decay can be treated independently of the excitation process. There too dynamic correlations may play a role: Resonant Auger decay may result in a kinetic energy shift of the emitted electron due to simultaneous transitions of valence electrons [4] and two [5,6] or three electrons [7] may be emitted in Auger decay of a single vacancy.

The most probable decay mode of a double vacancy is sequential relaxation, i.e., the core holes decay one after another going through a well-defined intermediate state. Another option had already been discussed when Schrödinger envisaged the possibility that a single photon is emitted in a concerted jump of two electrons that fill simultaneously the two vacancies [8]. For a double K vacancy the existence of such a two-electron one-photon (TEOP) decay was demonstrated 40 years ago by detection of K^2-M_1M_{23} x-ray lines in ion-atom collision experiments [9,10]. The TEOP experiment was recently performed by synchrotron light probing solid Mg, Al, and Si targets above their K^2-ionization thresholds [11].

Two inner vacancies can relax also by a correlated nonradiative decay, where a simultaneous jump down of two electrons is accompanied by emission of a single Auger electron. Similar to TEOP decay, such two-electron one-electron (TEOE) transitions result in spectral lines that are substantially blueshifted with respect to the characteristic lines of the corresponding sequential Auger decay. The feasibility of a TEOE transition had been discussed years before when Afrosimov *et al.* [12] reported the first experimental evidence for L^2 vacancy states. In an Ar^++Ar experiment a broad peak at 445 eV electron energy was interpreted as due to the three-electron L^2-M^3 transition starting from an average $2p^{-2}3p^{-2}$ configuration prepared by the collision process. Most of the early theoretical attempts concentrated on TEOE decay of a K^2 vacancy, starting with a shake-off model [13] and refining calculations using the many-body perturbation approach (MBPT) [14–17]. The calculated TEOE branching ratios are in the 10^{-4}–10^{-3} range and are consistent also with the results of electron capture experiments [18]. For L^2 vacancies Amusia and Lee [16] envisaged the existence of other than jump-down TEOE transitions and presented a general MPBT scheme to deal with them.

Although the available experimental data evidence the existence of the TEOE process, they are not yet of a spectroscopic quality, namely, in ion collision experiments the initial hollow state is not unambiguously defined and for a relatively small population of hollow atoms it is difficult to push the spectrometer resolving power below the natural linewidth of the core hole. It is nevertheless possible to prepare a substantial amount of well-defined double vacancy states by synchrotron light and actually perform the TEOE spectroscopy (Fig. 1).

We have measured a well-resolved L_{23}^2-M^3 TEOE spectrum in Ar and extracted the branching ratio with respect to the sequential Auger decay of the $L_{23}^2(^1D_2)$ vacancy. The experiment was performed at the GALAXIES beamline at SOLEIL synchrotron using the HAXPES Scienta R4000 hemispherical spectrometer collecting electrons within a 45° cone along the horizontal polarization direction of the incoming light [19]. The L^2 vacancy states were prepared by a single-photon K-shell ionization and subsequent K-L^2 decay. To characterize the population of L^2 states, the Ar K-L^2 spectrum (with satellites) was measured in the 2595–2680 eV energy range (Fig. 2). The TEOE spectra were recorded in the 415–480 eV energy range with a typical resolution of 150 meV and a 40-meV energy step (Fig. 1). Both the K-L^2 and the TEOE spectra were collected at two photon energies: at 3215 eV (above the K-edge threshold at 3206.2 eV and below the KM excitation threshold at 3221 eV) [Fig. 3(a)] and at 3900 eV [Fig. 3(b)].

In agreement with previous K-L^2 measurements [20,21], the spectra in Fig. 2 show that $2p^{-2}\,{}^1D_2$ is the most populated state of the Ar dication and that the transitions to $^1S_0$ and

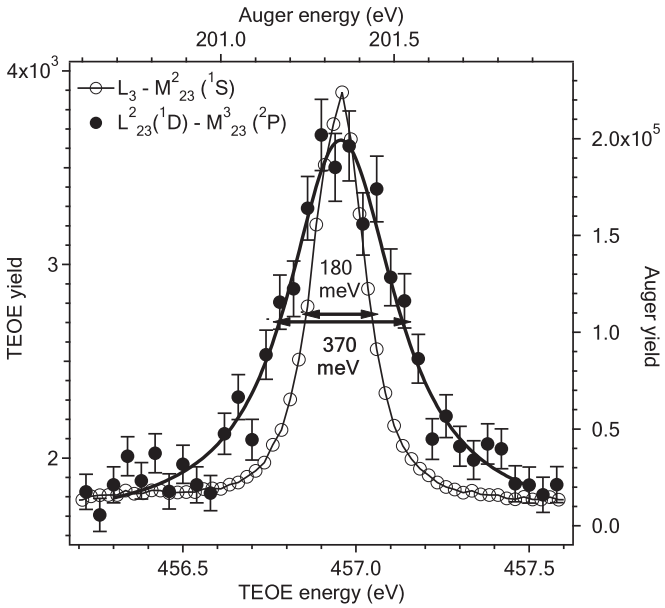

FIG. 1. The TEOE (closed circles) and the Auger (open circles) line, recorded with a spectral resolution of 104(5) meV.

$^3P_2$ states are much less probable [13(3)% and 1.2(2)%, respectively]. The recorded spectra are well reproduced by the calculated K-L^2 transition rates using asymmetric line profiles induced by postcollision interaction [22] (at 3215 eV) and accounting for the KM-L^2M satellite decay (at 3900 eV). The decay rate for the reaction $|\beta_i J_i \pi_i\rangle \rightarrow |\beta_f J_f \pi_f\rangle + e^-(\mathbf{k}_f)$ leading to emission of an Auger electron with energy $k_f^2/2$ was calculated with initial atomic i and final ionic f wave functions, represented by a linear combination of configuration-state functions (CSFs)

$$|\beta_i J_i \pi_i\rangle = \sum_\mu c_{i\mu} |\beta_\mu L_\mu S_\mu J_i \pi_i\rangle, \tag{1}$$

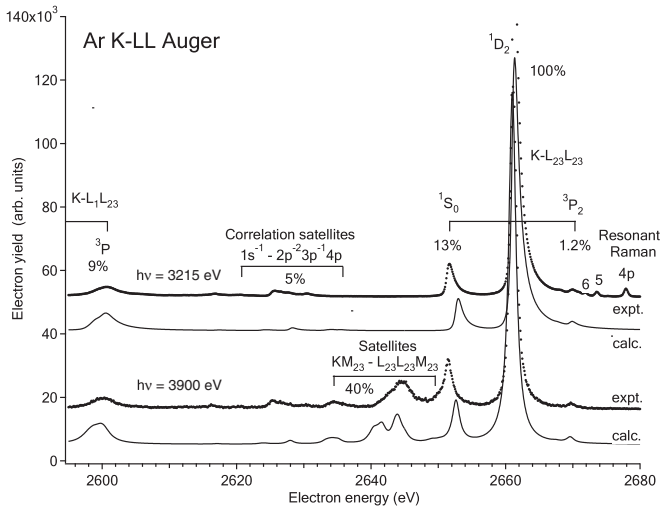

FIG. 2. Electron spectra in the energy region of K-L^2 Auger transitions in Ar recorded along the polarization direction of the incident light at photon energies of 3215 and 3900 eV (dots) compared to the calculated K-L^2 Auger spectra (line).

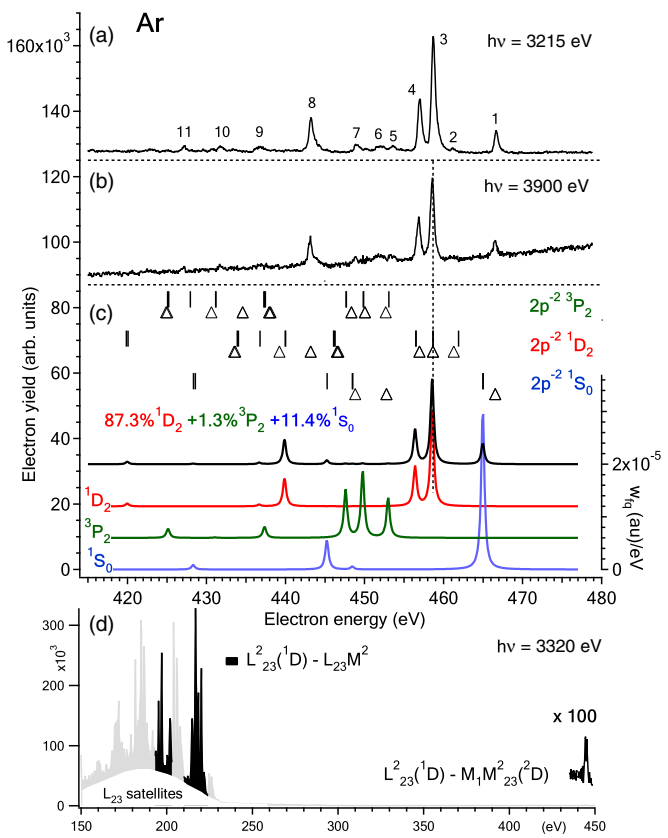

FIG. 3. Observed TEOE L_{23}^2-M^3 spectrum in Ar with the initial double vacancy prepared by K-L^2 Auger decay following photon absorption at (a) 3215 eV and (b) 3900 eV. (c) Calculated L_{23}^2-M^3 spectrum for ^1D (red curve), ^3P (green curve), and ^1S (blue curve) symmetry of L_{23}^2 together with the weighted sum to account for the initial vacancy population (black curve). Reported are the calculated transition energies (bars, shifted for -2.9 eV) and the transition energies (triangles) obtained from the previous data, as described in the text. (d) Broad range spectrum measured at 3320 eV photon energy.

$$|\beta_f J_f \pi_f\rangle |\chi_{\mathbf{k}_f}\rangle = \sum_\lambda c_{f\lambda} |\beta_\lambda L_\lambda S_\lambda J_f \pi_f\rangle \sum_{lj} a_{lj}^{\mathbf{k}_f} |l\tfrac{1}{2} j\rangle. \tag{2}$$

The parity of the state is denoted by π and the angular momentum J is a sum of orbital angular momentum L and spin S. The wave function of the continuum electron is expanded into partial waves $|l\frac{1}{2}j\rangle$. As single-photon absorption by the K-shell electron results in a zero alignment of the Ar^+ K^{-1} ion [23], the Auger decay rate integrated over the whole solid angle gives a measure of the K-L^2 signal

$$w_{if} = 2\pi \hat{J}_f \sum_{lj} \hat{j} \left| \sum_{\lambda\mu} \left[c_{i\mu} c_{f\lambda} \sqrt{\hat{L}_\mu \hat{S}_\mu} \begin{Bmatrix} L_\lambda & l & L_\mu \\ S_\lambda & \frac{1}{2} & S_\mu \\ J_f & j & J_i \end{Bmatrix} \right.\right.$$
$$\left.\left. \times \langle (\beta_\lambda L_\lambda S_\lambda) \left(k_f l \frac{1}{2} \right) L_\mu S_\mu || V || \beta_\mu L_\mu S_\mu \rangle \right] \right|^2. \tag{3}$$

The reduced matrix elements of the Coulomb interaction $V = \sum_{i>j} 1/r_{ij}$ were calculated according to [24] using large components of bound and continuum relativistic electron

orbitals obtained by the multiconfiguration Dirac-Fock model [25]. The abbreviation $\hat{j}$ is used for $2j+1$ and curly brackets denote the Wigner 9-j symbol.

Knowing the initial population of double L vacancies, we proceed to interpret the measured TEOE spectra. First, the positions of spectral lines are obtained by subtracting previously reported energies of the initial L^2 [20,26] and final V^3 valence states [27–30] in Ar. A comparison with the observed positions in Table I shows that most of the TEOE signal may indeed be attributed to the decay of the $L_{23}^2(^1D_2)$ vacancy, which is preferentially populated by K-L^2 decay.

The TEOE decay rates were calculated within the simplest MBPT model using a sequence of two electron-electron Coulomb interactions [31]. The spectral distribution is proportional to the angle-integrated TEOE decay rate

$$w_{fq} = 2\pi \hat{J}_q \hat{L}_i^3 \hat{S}_i^3 \sum_{lj} \hat{j} \left[\begin{Bmatrix} L_q & l & L_i \\ S_q & \frac{1}{2} & S_i \\ J_q & j & J_i \end{Bmatrix}^2 \left| \sum_p \hat{J}_p \sum_{l'j'} \hat{j}' \sum_{\lambda'\mu'} c_{p\lambda'} c_{p\mu'} \begin{Bmatrix} L_{\lambda'} & l' & L_i \\ S_{\lambda'} & \frac{1}{2} & S_i \\ J_p & j' & J_i \end{Bmatrix} \begin{Bmatrix} L_{\mu'} & l' & L_i \\ S_{\mu'} & \frac{1}{2} & S_i \\ J_p & j' & J_i \end{Bmatrix} \right.$$
$$\left. \times \int d\epsilon' \frac{\langle \beta_q L_q S_q \epsilon l \| V \| \beta_{\lambda'} L_{\lambda'} S_{\lambda'} \epsilon' l' \rangle \langle \beta_{\mu'} L_{\mu'} S_{\mu'} \epsilon' l' \| V \| \beta_f L_f S_f \rangle}{E_p + \epsilon' - E_f + i0^+} \right|^2 \Bigg]. \quad (4)$$

This formula assumes a single CSF representation of the initial bound state $|\beta_f J_f \pi_f\rangle$ with energy E_f and the same for the bound part $|\beta_q J_q \pi_q\rangle$ of the final state, which includes also a TEOE electron with energy $\epsilon = E_f - E_q$. A summation over the bound intermediate states of type (1) is omitted because it gives a negligible contribution compared to the type (2) states with energy $E_p + \epsilon'$.

TABLE I. Energies, spectral intensities, and assignment of the observed TEOE transitions. The experimental energy scale is shifted by −1.2 eV to match the energy of the $2p^{-2}\,{}^1D_2$–$3p^{-3}\,{}^2D$ transition (bold) extracted from the previous data, as described in the text. The TEOE decay rates w_{fq} are calculated according to (4). The experimental relative line intensities are compared with the calculated intensities that take into account the $^1D_2$:$^1S_0$:$^3P_2$ = 1:0.130:0.012 L_{23}^2 population ratio.

No.	ϵ[a] (eV)	Intensity[b] (%)	TEOE transition	ϵ[c] (eV)	w_{fq} (10^{-7} a.u.)	Intensity[d] (%)
1	466.61	18	$^1S_0$-$3p^{-3}\,{}^2P$	466.54	237	21
2	461.16	1	$^1D_2$-$3p^{-3}\,{}^4S$	461.28	0	0
3	**458.65**	100	$^1D_2$-$3p^{-3}\,{}^2D$	**458.65**	145	100
4	456.93	46	$^1D_2$-$3p^{-3}\,{}^2P$	456.94	59	41
5	453.55	5	$^1S_0$-$3s^{-1}3p^{-2}\,{}^2D$	452.78	4	1
			$^3P_2$-$3p^{-3}\,{}^4S$	452.67	59	
6	452.00	4	$^3P_2$-$3p^{-3}\,{}^2D$	450.05	100	1
7	448.94	7	$^1S_0$-$3s^{-1}3p^{-2}\,{}^2S$	448.83	44	6
			$^3P_2$-$3p^{-3}\,{}^2P$	448.34	69	
8	443.18	31	$^1D_2$-$3s^{-1}3p^{-2}\,{}^2D$	443.18	42	29
9	436.74	5	$^1D_2$-$3s^{-1}3p^{-2}\,{}^2S$	439.23	3	2
10	431.73	4	$^1S_0$-$3s^{-2}3p^{-1}\,{}^2P$	428	7	1
11	427.13	4	$^1D_2$-$3s^{-2}3p^{-1}\,{}^2P$	425.03	4	3

[a]Experimental energy scale.
[b]Experimental relative line intensity.
[c]From previous data.
[d]Calculated intensity.

To model the TEOE spectrum the following reaction paths were considered:

$$2p^{-2} \begin{cases} \nearrow \\ \rightarrow \\ \searrow \end{cases} \begin{matrix} 2p^{-1}3p^{-2}\epsilon' p \\ 2p^{-1}3p^{-1}3s^{-1}\epsilon'(s,d) \\ 2p^{-1}3s^{-2}\epsilon' p \end{matrix} \begin{cases} \rightarrow \\ \searrow \\ \rightarrow \end{cases} \begin{matrix} 3p^{-3}\epsilon p \\ 3s^{-1}3p^{-2}\epsilon(s,d) \\ 3s^{-2}3p^{-1}\epsilon p. \end{matrix} \quad (5)$$

The f partial waves give negligible contribution. The calculated TEOE rates are gathered in Table I and the model spectra are presented in Fig. 3(c) for the three L_{23}^2 symmetries. Their sum, weighted according to the initial vacancy population, agrees well with the observed signal [Figs. 3(a) and 3(b). The peak in row 2 with 1% relative intensity is clearly observed in Fig. 3(a) but not present in Fig. 3(c) because the $L_{23}^2(^1D_2)$-$M_{23}^3(^4S)$ transition is forbidden in the single-configuration model due to spin conservation. The CSF mixing reveals that the $^4S_{3/2}$ state acquires a small admixture of $^2P_{3/2}$ due to the spin-orbit interaction, which explains the observation. Since there is no significant difference between the TEOE spectra recorded at 3215 eV [Fig. 3(a)] and 3900 eV photon energies [Fig. 3(b)], we conclude that a TEOE process starting from the $L_{23}^2 M_{23}$ hollow states (40% relative population) is less probable than the TEOE decay of L_{23}^2, unless the satellite signal is dispersed over an extended spectral region.

In Fig. 1 the L_3-$M_{23}^2(^1S)$ Auger signal is compared with the TEOE $L_{23}^2(^1D_2)$-$M_{23}^3(^2P)$ signal. First, the respective linewidths reflect the lifetimes of a single L_3 and of a double L_{23}^2 vacancy, because in both cases any further decay is much slower. The full width at half maximum of the Lorentzian component in the fitted Voigt profile is 117(5) and 323(15) meV, respectively, leading to the lifetime ratio of 2.76(25). Similar to the K^2 vacancy case [32], a L_{23}^2 vacancy in Ar decays more than two times faster than a single L_3 vacancy. This is supported by the calculation of Auger transition rates of the corresponding dominant decay channels L_{23}^2-$L_{23}M^2$ and L_3-M^2. Using Eq. (3) with orbitals optimized for the initial $2p^{-2}$ configuration results in 30% (L_3) and 40% (L_{23}^2) overestimation of the linewidth and gives a 10% too large lifetime ratio.

Second, the branching ratio of a specific TEOE transition $L_{23}^2(^1D_2)$-$M_{23}^3(^2P)$ is determined (row 4 in Table I). To that purpose we employ the measured ratio $R = 2.0 \times 10^{-2}$ of line intensities in Fig. 1, which are normalized to the same photon flux, acquisition time, and electron transmission. The branching ratio is then given by

$$R\frac{\sigma_{L_3}(2300\text{ eV})}{\sigma_K(3900\text{ eV})}\frac{B\left[L_3\text{–}M_{23}^2\,{}^1S_0\right]}{B\left[K\text{–}L_{23}^2\,{}^1D_2\right]} \approx 5.6(10) \times 10^{-4}, \quad (6)$$

where 0.14 is the ratio of L_3 and K photoabsorption cross sections σ and 0.082 [33] and 0.42 [20,34] are the branching ratios B for transition with the initial L_3 and K vacancies, respectively. The partial photoabsorption cross sections at photon energies of 2300 and 3900 eV were obtained by interpolation of data tabulated in [35]. Relying on identification of TEOE spectral lines and on the measured relative line intensities in Table I, (6) leads to the experimental value of the TEOE branching ratio $X = 2.2(4) \times 10^{-3}$ for the double vacancy state $L_{23}^2(^1D_2)$.

An independent verification of this result was performed by a direct comparison of the TEOE $L_{23}^2(^1D_2)$-$M_1M_{23}^2(^2D)$ spectral intensity (row 8 in Table I) with the total spectral intensity of the predominant $L_{23}^2(^1D_2)$-$L_{23}M^2$ Auger decay channel. Both signals were recorded in the same broad range electron spectrum taken at 3320 eV photon energy [Fig. 3(d)]. This approach is more straightforward because it does not require knowledge of either the partial photoabsorption cross sections or the specific Auger branching ratios, except for the measured TEOE branching. On the other hand, its accuracy depends on precise isolation of the $L_{23}^2(^1D_2)$-$L_{23}M^2$ Auger signal, the first step in the sequential decay of the L_{23}^2 double core hole. This is one of the four main partially overlapping discrete spectral contributions in the 200-eV electron energy range where one also finds the LM^2-M^4 Auger signal, the L-M^2 Auger signal, and the LM-M^3 satellite signal enhanced due to Coster-Kronig decay of the L_1 vacancy. In addition, above the K-ionization threshold a strong and smooth satellite background appears due to Auger decay of KM vacancies and additional Coster-Kronig L_1-L_{23} vacancy transfer [36]. We have identified the $L_{23}^2(^1D)$-$L_{23}M^2$ part of the signal [marked by the black area in Fig. 3(d)] in comparison to the calculated Auger spectrum, taking into account the actual L_{23}^2 vacancy population ratio that favors the ^1D symmetry (Fig. 1).

We note that an old experimental value of Afrosimov *et al.* [12] is about about five times lower than X. The difference might be ascribed to the absence of some valence electrons in the initial TEOE state of the ion experiment and possibly to an overestimation of the L_{23}^2-$L_{23}M^2$ Auger cross section extracted from the ion collision data: The Auger signal in the poorly resolved 200-eV spectral region strongly overlaps with the signal of L_{23} satellites, which are rather intense already in the photoabsorption experiment [Fig. 3(d)].

The calculated decay rates give a theoretical estimate for the branching ratio: $X_{\text{MBPT}} = 1.4 \times 10^{-3}$. The agreement with the experimental value comes within the error bars (2.0×10^{-3}) when the measured L_{23}^2 vacancy width is inserted instead of the calculated one. We note that while the relative TEOE rates are quite insensitive to the chosen set of orbitals, their absolute values strongly depend on the selection. It turns out that the use of orbitals optimized for the initial $2p^{-2}$ configuration results in the largest TEOE rates and gives the best agreement with the experimental data. This is not surprising because the final electron rearrangement involves a substantial energy transfer that must occur before the first emitted electron escapes the atom.

It is interesting to compare our results with the results of the sudden approximation (SA), which was used previously to estimate the K^2-L^3 decay branching ratio in N^{M+} ions [37]. According to the SA, the second $2p$ vacancy is filled by the shake-down transition of the $3p$ electron due to the sudden change of the ionic potential caused by the L_{23}^2-$L_{23}M^2$ Auger decay. The intensity ratio of the two strongest lines in the TEOE spectrum (row 4 and row 3 in Table I) is then given by

$$\frac{\sum_q |\langle 2p^{-2}(^1D)|V|q(^2P)\epsilon p\rangle|^2 |\langle q|3p^{-3}(^2P)\rangle|^2}{\sum_r |\langle 2p^{-2}(^1D)|V|r(^2D)\epsilon p\rangle|^2 |\langle r|3p^{-3}(^2D)\rangle|^2} \approx 0.38, \quad (7)$$

where $|q\rangle$ and $|r\rangle$ denote the $2p^{-1}3p^{-2}$ intermediate ionic states coupled to ^2P and ^2D, respectively, with orbitals optimized for the initial $2p^{-2}$ configuration. As required by the SA, the orbitals of the final $3p^{-3}$ configuration are optimized for the $2p^{-1}3p^{-2}$ configuration to provide the nonzero overlap integrals. The result (7) is quite close to the MBPT ratio (0.41) and to the observed ratio (0.46). However, looking at the reaction scheme (5), it is clear that except for the $3p^{-3}$ final state, the configurations in the intermediate state interfere and along some of the reaction paths there is a switching of the partial continuum wave.

Rather than push the SA model too far we simplify the picture by estimating the TEOE branching ratio by $X_{\text{SA}} \approx |\langle 2p|3p\rangle|^2$. This is the same as assuming an equal value of the overlap integral for all the intermediate and final CSFs. Optimizing the $2p$ radial orbital by an average level calculation [25] involving $2p^{-1}(3p^{-2},3p^{-1}3s^{-1},3s^{-2})$ configurations results in $X_{\text{SA}}(\text{Ar}) \approx 2.6 \times 10^{-3}$, which is close to the experimental value. Unfortunately, the overlap integral value is quite sensitive to the choice of orbitals, namely, a reduction of X_{SA} for a factor of 3 occurs when the $2p$ orbital is optimized for the $2p^{-1}3p^{-2}$ configuration only. As the best optimization frame is not known *a priori*, the SA model is expected to be accurate to within a factor of 2 [37]. In a similar fashion we have also considered the L_{23}^2-M^3 case in Kr and obtained $X_{\text{SA}}(\text{Kr}) \approx 3.3 \times 10^{-4}$. Since the $X_{\text{SA}}(\text{Kr})/X_{\text{SA}}(\text{Ar})$ ratio turns out to be quite stable if calculated with the same optimization scheme, we estimate the TEOE branching ratio in Kr to be 6–8 times smaller than in Ar. This is not unexpected because in Kr a sudden change of the potential upon filling a $2p$ vacancy is relatively small due to the stronger electrostatic potential of the nucleus.

In conclusion, due to an efficient preparation of double vacancies by K-L^2 Auger decay driven by K-shell photoionization, we have clearly observed the L_{23}^2-M^3 transitions in Ar. The TEOE decay is a minor relaxation channel of the L_{23}^2 vacancy with a $2.2(4) \times 10^{-3}$ branching ratio. The well-resolved experimental spectra are closely reproduced by the second-order perturbation model when the population of initial double vacancies is taken into account. We have shown that modern instrumentation permits the acquisition of TEOE

spectra in a reasonable time and with experimental resolution better than the natural linewidth of the core-hole state. Finally, the application of TEOE spectroscopy to other (than) atomic targets seems straightforward and considerable chemical sensitivity is expected when valence electrons partake in the decay.

This work was supported by the P1-0112 research program of the Slovenian Research Agency. Experiments were performed at the GALAXIES beamline at SOLEIL Synchrotron, France (Proposal No. 99140145). We are grateful to SOLEIL staff for smoothly running the facility.

[1] C. Beilmann, P. H. Mokler, S. Bernitt, C. H. Keitel, J. Ullrich, J. R. C. López-Urrutia, and Z. Harman, Phys. Rev. Lett. **107**, 143201 (2011).

[2] J. Colgan, A. Emmanouilidou, and M. S. Pindzola, Phys. Rev. Lett. **110**, 063001 (2013).

[3] M. Nakano, F. Penent, M. Tashiro, T. P. Grozdanov, M. Žitnik, S. Carniato, P. Selles, L. Andric, P. Lablanquie, J. Palaudoux, E. Shigemasa, H. Iwayama, Y. Hikosaka, K. Soejima, I. H. Suzuki, N. Kouchi, and K. Ito, Phys. Rev. Lett. **110**, 163001 (2013).

[4] M. Meyer, E. von Raven, B. Sonntag, and J. E. Hansen, Phys. Rev. A **49**, 3685 (1994).

[5] T. A. Carlson and M. O. Krause, Phys. Rev. Lett. **14**, 390 (1965).

[6] Y. Hikosaka, P. Lablanquie, F. Penent, P. Selles, T. Kaneyasu, E. Shigemasa, J. H. D. Eland, and K. Ito, Phys. Rev. A **80**, 031404 (2009).

[7] A. Müller, A. Borovik, T. Buhr, J. Hellhund, K. Holste, A. L. D. Kilcoyne, S. Klumpp, M. Martins, S. Ricz, J. Viefhaus, and S. Schippers, Phys. Rev. Lett. **114**, 013002 (2015).

[8] E. Schrödinger, Z. Phys. **32**, 841 (1925).

[9] W. Wölfli, C. Stoller, G. Bonani, M. Suter, and M. Stöckli, Phys. Rev. Lett. **35**, 656 (1975).

[10] J. Volpp, R. Schuch, G. Nolte, and H. Schmidt-Bocking, J. Phys. B **12**, L325 (1979).

[11] J. Hoszowska, J.-C. Dousse, J. Szlachetko, Y. Kayser, W. Cao, P. Jagodziński, M. Kavčič, and S. H. Nowak, Phys. Rev. Lett. **107**, 053001 (2011).

[12] V. V. Afrosimov, Y. S. Gordeev, A. N. Zinov'ev, D. K. Rasulaov, and A. P. Shergin, J. Exp. Theor. Phys. Lett. **21**, 249 (1975).

[13] V. M. Kishinevski, V. I. Matveev, and E. S. Parilis, Pis. Zh. Tekn. Fiz. **12**, 810 (1976).

[14] L. N. Ivanov, U. I. Safronova, V. S. Senashenko, and D. S. Viktorov, J. Phys. B **11**, L175 (1978).

[15] R. L. Simons, H. P. Kelly, and R. Bruch, Phys. Rev. A **19**, 682 (1979).

[16] M. Y. Amusia and I. S. Lee, J. Phys. B **24**, 2617 (1991).

[17] J. P. Marques, F. Parente, P. Indelicato, and J. P. Desclaux, J. Phys. B **31**, 2897 (1998).

[18] L. Folkerts, J. Das, S. Bergsma, and R. Morgenstern, Phys. Lett. A **163**, 73 (1992).

[19] D. Céolin *et al.*, J. Electron Spectrosc. Relat. Phenom. **190**, 188 (2013).

[20] L. Asplund, P. Kelfve, B. Blomster, H. Siegbahn, and K. Siegbahn, Phys. Scr. **16**, 268 (1977).

[21] M. O. Krause, Phys. Rev. Lett. **34**, 633 (1977).

[22] B. Paripás, G. Vitéz, G. Víkor, K. Tökési, A. Caló, R. Sankari, M. Huttula, S. Aksela, and H. Aksela, J. Phys. B **37**, 4507 (2004).

[23] N. M. Kabachnik and I. P. Sazhina, J. Phys. B **17**, 1335 (1984).

[24] O. Zatsarrinny, Comput. Phys. Commun. **98**, 235 (1996).

[25] K. Dyall, I. Grant, C. Johnson, F. Parpia, and E. Plummer, Comput. Phys. Commun. **55**, 425 (1989).

[26] M. Deutsch, N. Maskil, and W. Drube, Phys. Rev. A **46**, 3963 (1992).

[27] E. B. Saloman, J. Phys. Chem. Ref. Data **39**, 033101 (2010).

[28] V. Kaufman and W. Whaling, J. Res. Natl. Inst. Stand. Technol. **101**, 691 (1996).

[29] J. E. Sansonetti and W. C. Martin, J. Phys. Chem. Ref. Data **34**, 1559 (2005).

[30] I. Velchev, W. Hogervorst, and W. Ubachs, J. Phys. B **32**, L511 (1999).

[31] V. Averbukh and P. Kolorenč, Phys. Rev. Lett. **103**, 183001 (2009).

[32] M. H. Chen, Phys. Rev. A **44**, 239 (1991).

[33] H. Pulkkinen, S. Aksela, O.-P. Sairanen, A. Hiltunen, and H. Aksela, J. Phys. B **29**, 3033 (1996).

[34] M. O. Krause, Phys. Rev. Lett. **34**, 633 (1975).

[35] J. Scofield, Technical Report UCRL-51326, Lawrence Livermore National Laboratory, 1973.

[36] U. Arp, T. LeBrun, S. H. Southworth, M. A. MacDonald, and M. Jung, Phys. Rev. A **55**, 4273 (1997).

[37] N. Vaeck and J. E. Hansen, J. Phys. B **25**, 3613 (1992).